INTERNATIONAL JOURNAL FOR NUMERICAL METHODS IN FLUIDS
Int. J. Numer. Meth. Fluids 2010; **62**:733–746
Published online 27 July 2009 in Wiley InterScience (www.interscience.wiley.com). DOI: 10.1002/fld.2038

Two-dimensional modeling for stability analysis of two-phase stratified flow

Ghassem Heidarinejad*,† and Abdollah Eskandari Sani

Department of Mechanical Engineering, Tarbiat Modarres University, Tehran, Iran

SUMMARY

The effect of wavelength and relative velocity on the disturbed interface of two-phase stratified regime is modeled and discussed. To analyze the stability, a small perturbation is imposed on the interface. Growth or decline of the disturbed wave, relative velocity, and surface tension with respect to time will be discussed numerically. Newly developed scheme applied to a two-dimensional flow field and the governing Navier–Stokes equations in laminar regime are solved. Finite volume method together with non-staggered curvilinear grid is a very effective approach to capture interface shape with time. Because of the interface shape, for any time advancement, a new grid is performed separately on each stratified field, liquid, and gas regime. The results are compared with the analytical characteristics method and one-dimensional modeling. This comparison shows that solving the momentum equation including viscosity term leads to physically more realistic results. In addition, the newly developed method is capable of predicting two-phase stratified flow behavior more precisely than one-dimensional modeling. It was perceived that the surface tension has an inevitable role in dissipation of interface instability and convergence of the two-phase flow model. Copyright © 2009 John Wiley & Sons, Ltd.

Received 2 December 2008; Revised 8 February 2009; Accepted 9 February 2009

KEY WORDS: two-dimensional modeling; stability; two-phase flow; stratified flow; non-staggered grid; curvilinear coordinate

1. INTRODUCTION

Two-phase flow is a common observation such cases occur in evaporation, condensation, cooling tube, phase changes, and boiling of liquids. However, a usual phenomenon in industrial application is stratified two-phase flow that happens when two different fluids are transferred simultaneously

*Correspondence to: Ghassem Heidarinejad, Department of Mechanical Engineering, Tarbiat Modarres University, Tehran, Iran.
†E-mail: gheidari@modares.ac.ir

through a channel. This situation also occurs at power plant cooling system in which an incorrect estimation could lead to slug regime and tube burning. Stratified flow is considered a basic flow configuration in horizontal and inclined two-phase systems of a finite density differential. Models of stratified flow are important from a technical point of view, as they are often met in industrial plants. From the hydraulic point of view, a two-phase flow in a duct is modeled to predict the flow characteristics, including pressure drop, holdup, and are often used as a starting point in modeling flow patterns transitions. The common assumption is that the interface separating the phases is a plane. This assumption is appropriate for gravity-dominated systems, such as large-scale gas–liquid horizontal flows under earth's gravity. In reduced gravity systems, capillary systems or in the case of low-density differential (such as oil–water systems), surface forces become important. The wetting fluid tends to climb over the tube wall resulting in a curved (convex or concave) interface. Stratified flows with curved interfaces in gas–liquid systems are observed both in experiment and numerical simulations [1]. A configuration of a curved interface is associated with a different contact area between the two fluids and between the fluids and the pipe wall. Depending on the physical system involved, these variations can have prominent effects on the pressure drop and transport phenomena. In order to prevent further complication in numerical modeling, usually a rectangular two-dimensional duct passage is considered. Therefore, the flow regime is considered one-dimensional and parallel to the duct length. Once the location of the fluid interface is known, then a two-dimensional velocity profile in a steady and fully developed axial laminar flow of stratified layers is obtained via analytical or numerical method [2].

In this paper, each fluid phase is solved independently. The required boundary conditions follow from the no-slip condition at the pipe wall and continuity of the velocities. The surface tension effect across the fluid's interface is considered as a coupling equation to link two sets of equation. A simple calculation for horizontal fully developed flow shows that Navier–Stokes in vertical direction yields a linear variation of the pressure in this direction due to the hydrostatic pressure. For axial, fully developed flow, the hydrodynamic stresses normal to the fluids interface vanish. In this case, the equation for the interface location evolves from the condition of equilibrium between the pressure jump across the interface and the surface tension force.

The effect of the wave generated on the interface of fluids, relative velocity, and surface tension is taken into consideration. Therefore, a small disturbance—a sinusoid curve—initially introduced on the interface. As time increases, depending on the relative velocity of two phases and nature of fluids, the disturbance would grew up or tend to level out. This condition can be taken into consideration for stability or instability criterion.

2. GEOMETRICAL CONSIDERATION

As stressed earlier, to capture interface shape more precisely, the pressure value near the surface shall be determined as accurately as possible. In the previous work, [3] at each section, the pressure average for liquid and gas flow was calculated. Although this simplification leads to a straightforward simulation of the flow field and results in overall estimation of interface shape, but it cannot evaluate the instability condition and onset of slug formation as exactly as required. Furthermore, the viscosity term of Navier–Stokes equation was added to equation of Characteristics model [4]. So, the grid of the flow field for each phase was separately generated. Because of interface variation at each time step, grid arrangement is adapted to new geometry. Hence, the

DOI: 10.1002/fld

system of equations shall be solved in a curvilinear coordinate. To solve the Navier–Stokes equation for each phase, we used a Cartesian velocity component in strong conservation form which when used together with a finite volume method, automatically ensures the global momentum conservation during the course of calculation [5]. The use of Cartesian velocity components as the primary dependent variables has also the advantages that the governing equations remain in a simple form. On the other hand, the use of covariant or contra variant velocity components (or volume fluxes) results in extra sources terms and more complicated equation. At any time advancement, four equations—in horizontal and vertical direction—are to be solved, so the staggered grid method is time consuming. In two-dimensional problems, all two Cartesian velocities are defined on each control volume face resulting in the definition of six velocities and the solution of six momentum equation per control volume. Moreover, a spatial interpolation scheme needs to be used to prevent decoupling of covariant velocity components from the pressure field. The result shows that a staggered grid method in curvilinear coordinate may require a large amount of computer memory to store the matrices of variables. In other words, although the staggering of the velocity components is of huge benefit on rectangular meshes but the method does not extend easily to curvilinear coordinate. In the approach presented here, all quantities are solved and stored at the element center. The face values of the velocity components have to be calculated from these element-based values. This leads to the need to employ an alternative interpolation method, The Rhie–Chow interpolation method does not suffer from the checkerboard effect [6].

Because of the non-staggered grid layout, the accuracy of this method is not affected by grid orientation. Based on insights from the above, we have extended the non-staggered grid method, which was developed for steady single-phase flow to solve the time-dependent incompressible two-phase flow in curvilinear coordinate. In this method, the Cartesian components of velocity and pressure are computed at cell center while volume fluxes are determined on its corresponding faces. Figure 1 shows the non-staggered grid cell place of storing variables.

The governing equations and the coordinate transformation are presented in Section 3. The numerical method is described in Section 4.

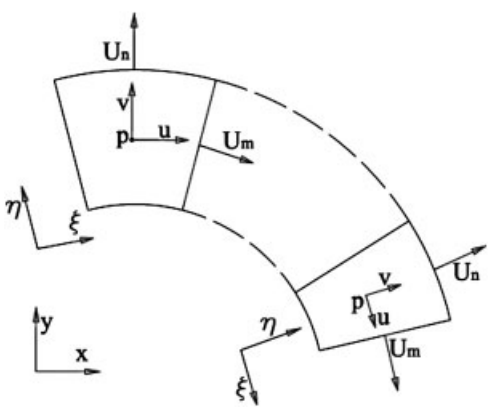

Figure 1. Non-staggered grid method; u, v: Cartesian velocity components; U, V: volume fluxes; p: pressure.

DOI: 10.1002/fld

3. GOVERNING EQUATIONS

The governing equation for each phase with constant viscosity and density as follows:

$$\frac{\partial u_i}{\partial x_i} = 0.0, \quad i = 1, 2 \tag{1}$$

$$\frac{\partial u_i}{\partial t} + \frac{\partial (u_i u_j)}{\partial x_j} = -\frac{\partial p}{\partial x_i} + \frac{\partial \tau_{ij}}{\partial x_j} + S, \quad i, j = 1, 2 \tag{2}$$

$$\tau_{ij} = v \frac{\partial u_i}{\partial x_j}, \quad i, j = 1, 2 \tag{3}$$

where u_i represents Cartesian velocity components, p is the flow field pressure divided by density of phases, v is kinematical viscosity of each phase, and S denotes the source term (e.g. gravity force). Equations (1)–(3) are similar for both gas and liquid flow field. For horizontal duct, it is assumed that the liquid occupies the lower section and the gas flows over the liquid as shown in Figure 2. Equations (1) and (2) are transformed into curvilinear coordinates as follows:

$$\frac{\partial U_m}{\partial \xi_m} = 0.0, \quad m = 1, 2 \tag{4}$$

$$\frac{\partial (J u_i)}{\partial t} + \frac{\partial (H_{im})}{\partial \xi_m} = 0.0, \quad m, i = 1, 2 \tag{5}$$

where H_{im} is

$$H_{im} = U_m u_i + J \frac{\partial \xi_m}{\partial x_i} p - v G^{mn} \frac{\partial u_i}{\partial \xi_n} - S, \quad m, i = 1, 2 \tag{6}$$

J is the Jacobean or the volume of the cell.

U_m is the volume flux normal to the cell surface of constant ξ_m and G^{mn} is the geometrical diffusion or mesh skewness tensor.

$$U_m = u_j A_j^m = J \frac{\partial \xi_m}{\partial x_j} u_j \tag{7}$$

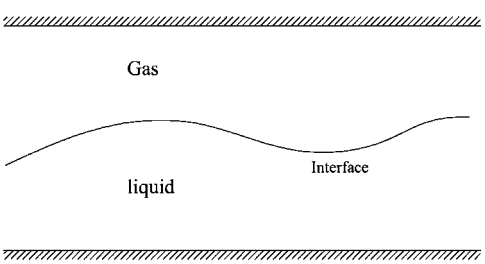

Figure 2. Schematic passage of liquid and gas phase and interface shape in the duct.

DOI: 10.1002/fld

$$J = \det\left(\frac{\partial x_i}{\partial \xi_j}\right) \tag{8}$$

$$G^{mn} = \frac{A^m A^n}{J} = J\frac{\partial \xi_m}{\partial x_j}\frac{\partial \xi_n}{\partial x_j} \tag{9}$$

Integrating Equations (1) and (2) over the cell volume and using Stokes theorem, and over the time step Δt, the following equations are obtained:

$$\sum_{c.s} U_m^{nn+1} = 0.0 \tag{10}$$

$$(u_i^{nn+1} - u_i^{nn})\cdot J - \left(-\frac{\partial p}{\partial \xi_j}\cdot\frac{\partial \xi_j}{\partial x_i}\right)_P \cdot J \cdot \Delta t + \sum_{c.s.}\left(U_m u_i - \nu G^{mn}\frac{\partial u_i}{\partial \xi_n}\right)^{nn}\cdot \Delta t + \int_t^{t+\Delta t} \overline{S}\cdot J\,\mathrm{d}t = 0.0 \tag{11}$$

where c.s. indicates that the summation is carried over the cell surfaces.

The superscript nn in equation above represents the time advancement.

4. NUMERICAL METHOD

As noted earlier, the shape of the interface at any time step dictates a curvilinear grid, which is discussed to be non-staggered. However, in order to solve equation in computational space it is aimed to be orthogonal with unit increment along the x and y direction, i.e. orthonormal space. Figure 3 shows the mapping of a skewed mesh onto orthonormal space.

When $m \neq n$, G^{mn} determines the mesh skewness. In other word, when the grid in physical space is orthogonal, the off-diagonal viscous terms will be vanished. Generally, this term has less significant contribution unless the grid is severely skewed and usually treated explicitly in order to yield a simple calculation [7]. However, in highly skewed mesh—in our problem when the slug

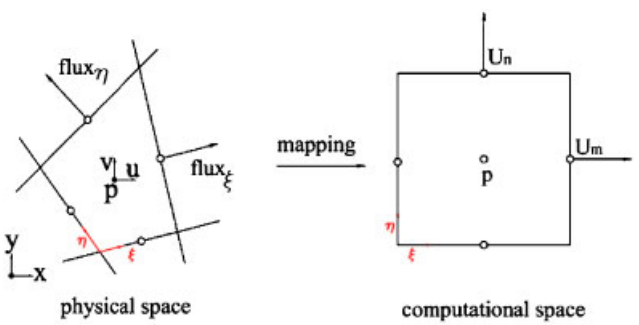

Figure 3. Orthonormal mapping of physical space onto computational space (we use to some extent, the notation of Robert and co-workers [7]).

DOI: 10.1002/fld

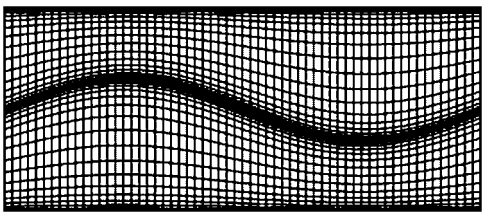

Figure 4. Clustering of mesh at the proximity of interface and walls (interface curvature shown exaggerated).

regime starts to be developed, the interface rises sharply and hence mesh skewness increases—it is necessary to reduce time step as much as possible. The convective terms are approximated using both quadratic upwind interpolations (QUICK) and second-order upwind scheme. Time advancing is considered explicit as it is described in Section 3. In order to capture precisely the flow structure near the wall and better handling of properties and flow characteristics near the interface, the grid has been clustered at the lower and upper of the duct and proximity of the interface using an exponential distribution, as shown in Figure 4.

5. PRESSURE TREATMENT

The Navier–Stokes equations are often integrated with respect to time using the fractional step procedure. This method was first proposed by Harlow and Welch [8]. In this method, the Navier–Stokes equation without pressure term is integrated to obtain an intermediate velocity field, which will in general not to be divergence free. Then a correction is applied to that velocity field to produce a velocity field, which satisfies in continuity equation. An orthogonal mapping from intermediate velocity field to divergence-free velocity field. This half stage in time advancing is called the projection step. It was shown that the time accuracy of projection method is first order [9]. There are two main reasons that the CPU time will be increased; first, solving two flow fields separately and second, the explicit time advancement, which is due to approximation of spatial term at previous time step. However, to reduce CPU time, a non-iterative projection method known as (P1) is used. In this method, the momentum equation is solved explicitly without pressure term. The intermediate velocity obtained in this stage is substituted in continuity equation, which yields Poisson equation. In P1 projection method, it is necessary to solve Poisson equation very accurately.

Consequently, the following steps shall be performed for any time advancement:

1. Prediction step: Solving Navier–Stokes equation without pressure gradient term:

$$\frac{u_i^* - u_i^{nn}}{(\Delta t/2)} J = \left[U_m u_i - \nu G^{mn} \frac{\partial u_i}{\partial \xi_n} \right]^{nn} \tag{12}$$

2. Poisson equation: Intermediate velocity u_i^* are substituted in Equation (4) to obtain Poisson equation

$$\frac{\delta}{\delta \xi_m} \left(G^{mn} \frac{\delta p^{nn+1}}{\delta \xi_n} \right) = \frac{1}{\Delta t} \frac{\delta U_m^*}{\delta \xi_m} \tag{13}$$

DOI: 10.1002/fld

In this relation, subscript denote time step, $*$ denote intermediate parameter, and δ is time and spatial discretization.

3. Correction step: The new velocity obtained using the correction equation:

$$\frac{u_m^{nn+1}-u_m^*}{\Delta t}=\frac{\partial p}{\partial \xi_m}\frac{\partial \xi_m}{\partial x_i} \tag{14}$$

There are few points to be considered to solve the Poisson equation. It is necessary to interpolate velocity at cell center and compute volume flux at faces, which is the source term of Equation (13). Since in P1 projection method the pressure term is ignored in momentum equation at prediction step, the checker-board condition will not occur; consequently it is not necessary to use non-linear interpolation. However, in order to achieve more precise results both second- and third-order interpolation are used. Another point is that because geometry diffusion is vanished for off-diagonal term in orthogonal coordinate, the boundary conation is zero gradient of pressure in direction perpendicular to wall. Nevertheless, for the present case in which the coordinate is not orthogonal, the boundary condition shall be derived using flux equation for cell adjacent to wall:

$$U_m^{nn+1}=U_m^*-\Delta t\left(G^{mn}\frac{\delta p^{nn+1}}{\delta \xi_n}\right) \tag{15}$$

when the boundary is a duct wall, volume flux is given, so U_m^{nn+1} is constant in time. The value of U_m^* is computed from u_m^* at cell face, which is extrapolated from the velocity at cell center Figure 5.

Since the flux is given at boundary, the boundary value for pressure is obtained from Equation (15). It should be noted that the flux value at the interface is zero, because it is assumed there is no mass transfer through the interface due to evaporation or condensation.

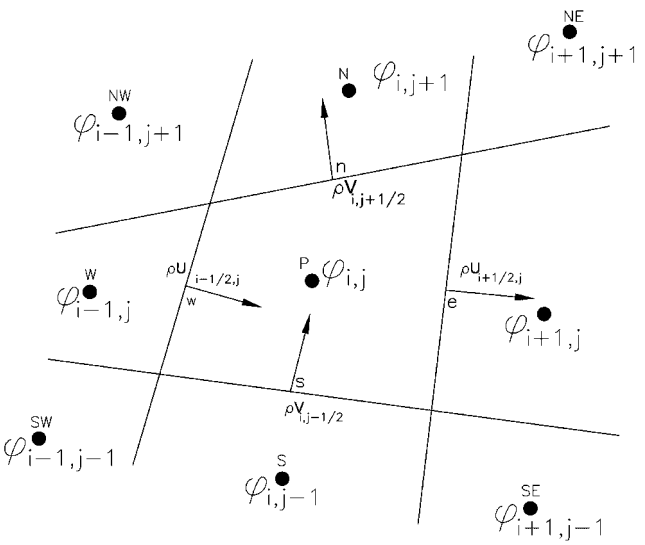

Figure 5. Calculation of volume flux near the boundary to obtain boundary condition.

DOI: 10.1002/fld

6. COUPLING OF TWO PHASES

As the flow field was computed for two phases using disturbed interface as the initial condition, the pressure values were obtained at the last grid point near the interface along the ducts. The pressure value is substituted in surface tension equation

$$\sigma = -\frac{\Delta P}{R} \tag{16}$$

where σ is the surface tension, R is interface curvature at any point, and ΔP is obtained from the following equation:

$$\Delta P = \rho_{\mathrm{l}} p_{\mathrm{l}} - \rho_{\mathrm{g}} p_{\mathrm{g}} \tag{17}$$

where p_{l} and p_{g} are the pressure of the last grid point value near the interface divided by density for liquid and gas, respectively. Figure 6 shows schematically the nearest node to interface.

After the pressure field is obtained, the curvature of interface can be estimated. For the next time step, the new shape of interface is the new boundary condition at the interface of two phases. The velocity boundary condition at interface is also considered so that the interface velocity is the average of two-phase velocity at on grid apart from interface i.e.:

$$V_{\mathrm{interface}} = 0.5(V_{\mathrm{liquid}} + V_{\mathrm{gas}}) \tag{18}$$

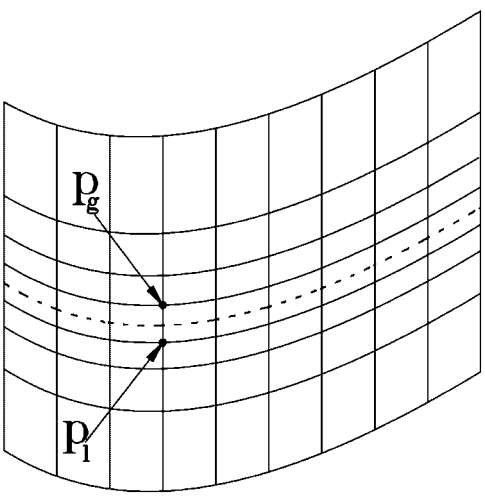

Figure 6. Last point position of phases near the interface for coupling system of equation.

DOI: 10.1002/fld

7. RESULTS

To investigate the stability condition of a two-phase flow, a channel with the length $L=1\,\mathrm{m}$, and height $H=0.1\,\mathrm{m}$, and initial void fraction (the volume ratio of gas to liquid) $\alpha_g=0.5$ is assumed ($\alpha_l=1-\alpha_g$). Liquid and gas are water and air with the following properties:

$$\rho_{water}=998\,\mathrm{kg/m^3},\quad \rho_{air}=0.995\,\mathrm{kg/m^3}$$

$$\mu_{water}=1.0\times10^{-3}\,\mathrm{kg/m\,s}$$

$$\mu_{air}=1.8\times10^{-5}\,\mathrm{kg/m\,s}$$

$$\sigma=0.0728\,\mathrm{N/m}$$

At the first step, for relative velocity $\Delta v=0.3\mathrm{m/s}$, ($\Delta v=v_{water}-v_{air}$) , a small sinusoid disturbance $\eta_0(x)=[\alpha_l+0.005\sin(2\pi x/\lambda)]$. H is introduced on the interface of two phases, which defines the initial shape of the interface. Here λ is the initial value of the wavelength. With time, the height of interface with respect to duct length, which is hereafter termed $\eta(x)$, decreased until it approaches to zero. The most important advantages of two-dimensional solution with respect to one-dimensional modeling considered here [3] is that one can trace the interface shape from onset of damping to full dissipation state. However, in one-dimensional modeling, only the onset of damping or growth of perturbation can be perceived.

As expected, because of relative velocity 0.3 m/s, the critical wavelength is about 1.26 m, so the imposed perturbation is dissipated, until it is completely damped ($\lambda<1.26\,\mathrm{m}$), Figure 7. The analytical relation for critical wave number k_c, in the notation of the present paper, is as follows [4]:

$$k_c=|\Delta v|\cdot[\rho_l\cdot\rho_g/\sigma H(\alpha_l\rho_g+\alpha_g\rho_l)]^{0.5} \tag{19}$$

So the critical wavelength, λ_c, is obtained as:

$$\lambda_c=2\pi/k_c \tag{20}$$

Variation of the critical wavelength versus relative velocity of two phases is shown in Figure 8, using the Equation (20).

Here, in addition to the onset time of damping time, one can trace the interface after it is completely dissipated, Figure 7.

With the same relative velocity, the perturbation wavelength has been changed to 0.5 m.

Figure 9 shows that as the wavelength decreases, the damping time also decreases.

In order to examine dissipation effects of viscosity, first, the relative velocity is assumed to be $\Delta v=1\,\mathrm{m/s}$. According to one-dimensional characteristics method, the critical wavelength will be about 0.38 m. But the interface shape shows that it tends to level out although it takes time longer than when $\Delta v=0.3\,\mathrm{m/s}$. Despite of the critical limit that is predicted by non-viscous modeling as shown in Figure 10, our new model predicts physically more accurate critical limit for perturbation wavelength. Strictly speaking, the critical wavelength, beyond which perturbation will grow, is slightly larger.

Compared with results obtained by non-viscous one-dimensional modeling, which has shown variation of $(\delta(\eta(x))=\eta(x)_{max}-\eta(x)_{min})$ with respect to time for different relative velocities, in the notation of the present paper, as perceived from Figure 11, the viscosity has an inevitable role in dissipation of interface instability; comparing with one-dimensional modeling in which the

DOI: 10.1002/fld

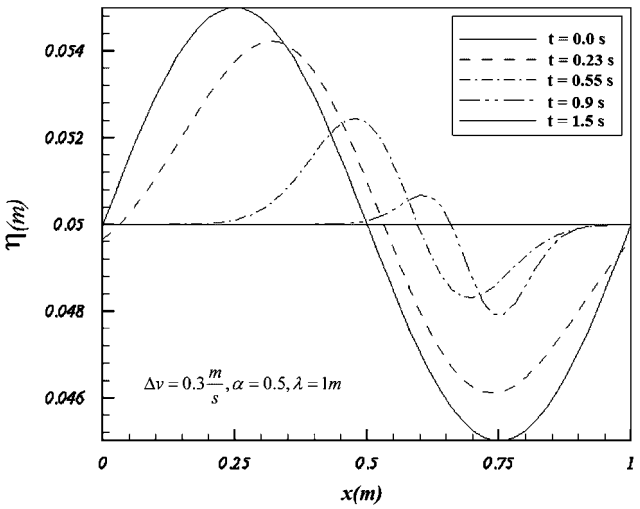

Figure 7. Dissipation of perturbation on interface ($\Delta v = 0.3\,\mathrm{m/s}$, $\alpha = 0.5$, $\lambda = 1\,\mathrm{m}$).

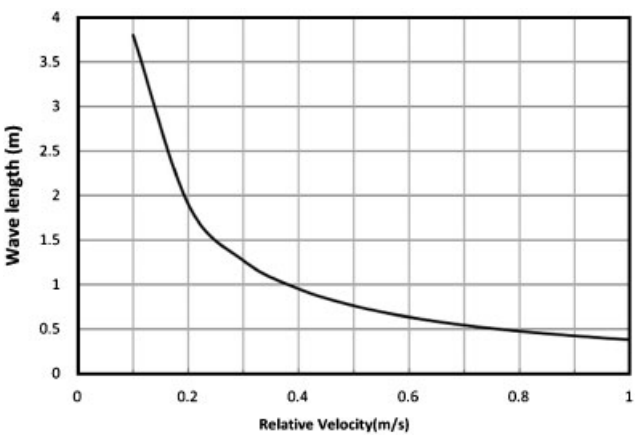

Figure 8. Critical wavelength with respect to relative velocity ($\sigma = 0.0728\,\mathrm{N/m}$).

viscosity was neglected, at the same time and after the initial state, the wave has been damped more.

To compare our results with the characteristic method approximation, a spatial growth of wave along the channel is computed and presented. As depicted in Figure 8, for a specific relative velocity if the wavelength is larger than a critical value, the perturbation will grow up. Based on Figure 8, for arbitrary value corresponding to an unstable region i.e. relative velocity $\Delta v = 0.5\,\mathrm{m/s}$ and wavelength $\lambda = 1.5\,\mathrm{m}$ perturbation grows; our results presented in Figure 12 also indicates growth of perturbation, however, the growth is less than corresponding one-dimensional model.

Present model (two-dimensional, including the surface tension and viscosity parameters) not only has more predictive capability but also establishes convergent results. The results obtained

DOI: 10.1002/fld

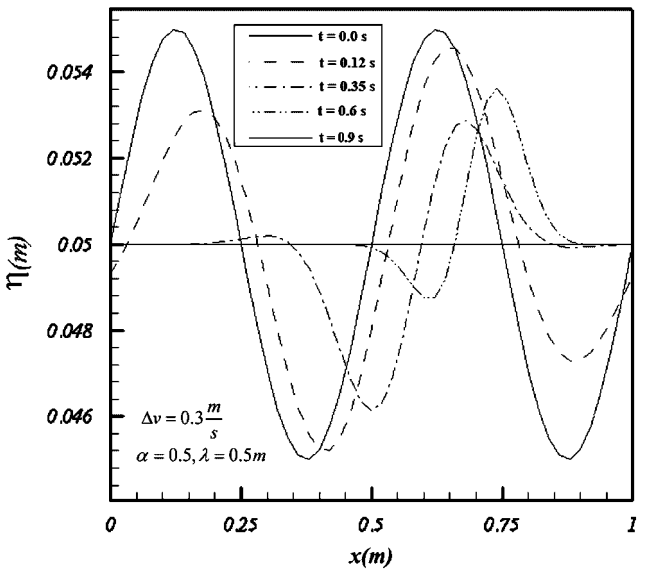

Figure 9. Dissipation of perturbation on interface ($\Delta v = 0.3\,\mathrm{m/s}, \alpha = 0.5, \lambda = 0.5\,\mathrm{m}$).

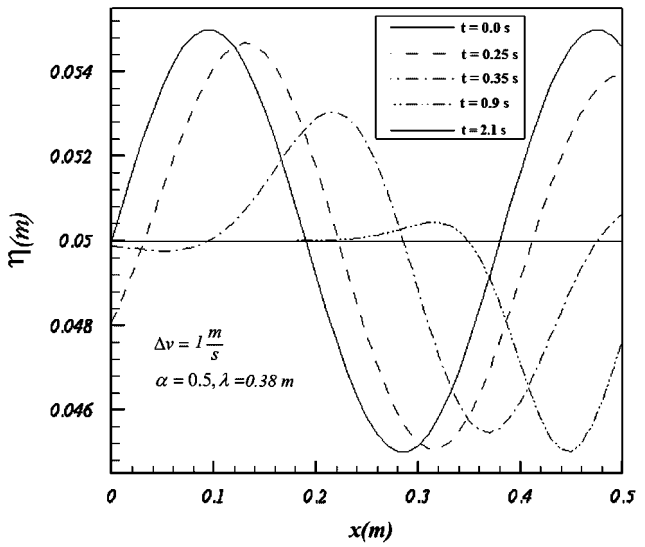

Figure 10. Dissipation of perturbation on interface ($\Delta v = 1\,\mathrm{m/s}, \alpha = 0.5, \lambda = 0.38\,\mathrm{m}$).

by such a model could lead to better modeling of the behavior of two-phase flow systems and hence to better system design and control. In order to verify the results obtained by the numerical method, the total number of mesh points, $n_x \times n_y$, where n_x and n_y are the number of mesh points in the parallel and perpendicular direction of duct length, respectively, was increased on the same

DOI: 10.1002/fld

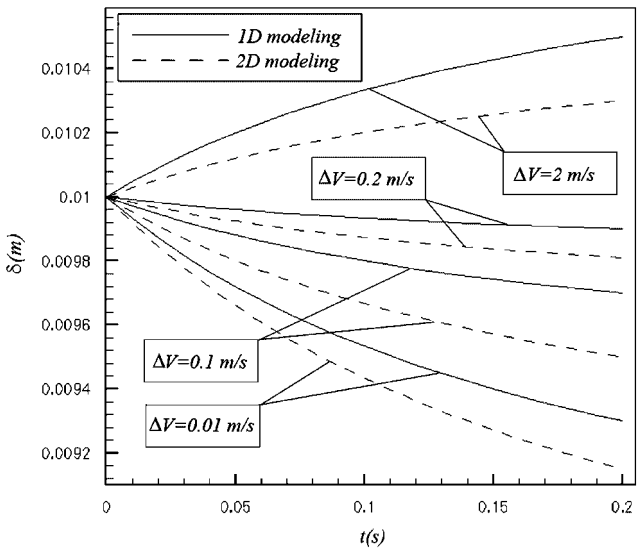

Figure 11. Comparison of one-dimensional and two-dimensional modeling of two phase flow ($\lambda = 1\,\text{m}, \alpha = 0.5, t = 0.2\,\text{s}$).

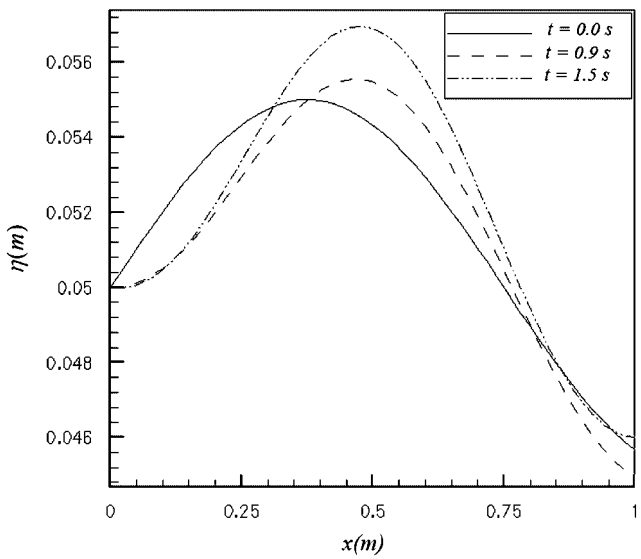

Figure 12. Perturbation growth for wavelength larger than critical value for a specific relative velocity ($\Delta v = 0.5\,\text{m/s}, \alpha = 0.5, \lambda = 1.5\,\text{m}$).

duct scale. The results indicating decay of the perturbations, $\delta(\eta(x))$, are presented in Figure 13. As it is obvious, when the mesh point's numbers were increased, convergence was obtained. The number of mesh points for each phase in the direction perpendicular to duct is the same and equal

DOI: 10.1002/fld

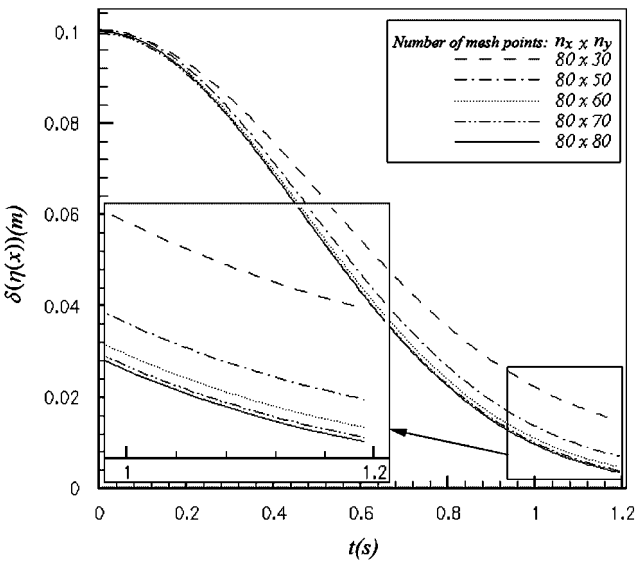

Figure 13. Grid independency; the difference for large number of mesh points is negligible.

to $n_y/2$. The difference between the results obtained for the total number of mesh points 80×70 and 80×80 is negligible.

8. CONCLUSION

It is shown that including viscous terms in Navier–Stokes equations makes the solution more realistic. Also using two-dimensional modeling helps to capture interface behavior as precisely as possible. In other words, the coupling pressure equation, which links two phases at interface, can be more effective when pressure of the nearest point to interface for each phase is used. As an important conclusion, two-dimensional modeling predicts critical wavelength slightly larger than that of one-dimensional modeling forecast. This conclusion is absolved with dissipation effects of viscosity terms. Also the increase in instability with increase in initial perturbation is the same as previous results although the value of critical wavelength is greater. Finally, it can be concluded that for the same instant after initial condition, the two-dimensional model predicts the growth or damping of the perturbation on the interface a little lesser than that of the one-dimensional model.

REFERENCES

1. Newton CH, Behnia M. A numerical model of stratified wavy gas–liquid pipe flow. *Chemical Engineering Science* 2001; **56**:6851–6861.
2. Newton CH, Behnia M. Estimation of wall shear stress in horizontal gas–liquid stratified flow. *American Institute of Chemical Engineers Journal* 1996; **42**:2369–2373.
3. Ansari MR, Sani AE. Surface tension effect on stability of two-phase stratified flow. *Fluid Dynamics Research* 2007; **39**:279–291.
4. Ramshaw JD, Trapp JA. Characteristics, stability and short wave length phenomena in two-phase flow equation system. *Nuclear Science Engineering* 1978; **66**:93–102.

DOI: 10.1002/fld

5. Ferziger JH, Peric M. *Computational Methods for Fluid Dynamics*. Springer: Berlin, Heidelberg, New York, 2002.
6. Rhie CM, Chow WL. Numerical study of the turbulent flow. Past an airfoil with trailing-edge separation. *AIAA Journal* 1983; **21**(11):1525–1532.
7. Zang Y, Street RL, Koseff JR. A non-staggered grid, fractional step method for tome-dependent incompressible Navier–Stokes equation in curvilinear coordinates. *Journal of Computational Physics* 1994; **114**:18–33.
8. Harlow F, Welch E. Numerical calculation of time-dependent viscous incompressible flow of fluid with free surface. *Physics of Fluids* 1965; **8**:2182–2189.
9. Armfield S, Street R. An analysis and comparison of the time accuracy of fractional-step methods for the Navier–Stokes equations on staggered grids. *International Journal for Numerical Methods in Fluids* 2002; **38**: 255–282.

DOI: 10.1002/fld